

## **Development of the High Strength Cold Worked Super Austenitic Stainless Steel UNS N08034 for Challenging Oilfield Environments**

Julia Botinha  
VDM Metals International GmbH  
Kleffstraße 23  
Altena, Nordrhein-Westfalen, 58097  
Germany

Helmuth Sarmiento Klapper  
Baker Hughes  
Baker-Hughes-Straße 1  
Celle, Niedersachsen, 29221  
Germany

Clara Herrera  
Deutsche Edelstahlwerke Specialty Steel  
GmbH & Co. KG  
Auestraße 4  
Witten, Nordrhein-Westfalen, 58452  
Germany

Merlin Seifert  
Deutsche Edelstahlwerke Specialty Steel  
GmbH & Co. KG  
Auestraße 4  
Witten, Nordrhein-Westfalen, 58452  
Germany

Bodo Gehrman  
VDM Metals International GmbH  
Kleffstraße 23  
Altena, Nordrhein-Westfalen, 58097  
Germany

Helena Alves  
VDM Metals International GmbH  
Kleffstraße 23  
Altena, Nordrhein-Westfalen, 58097  
Germany

### **ABSTRACT**

Corrosion resistant alloys are used in oilfield applications where carbon and low-alloy steels are expected to be affected by corrosion, and they often represent a cost-effective alternative to chemical treatment, or where specific application-driven requirements are required. Several alloys from 13% chromium stainless steel up to highly-alloyed nickel and cobalt alloys have been successfully used in drilling, completion, production as well as offshore oilfield equipment, where corrosion resistance is of concern. Many drilling technology components, for example, require non-magnetic austenitic stainless steels. In demanding production environments involving very corrosive fluids at elevated temperatures, on the other hand, nickel alloys are preferred. While one of the disadvantages of stainless steels concerns their limited resistance to localized corrosion and stress corrosion cracking in halide-containing environments, nickel alloys, particularly those that are precipitation hardenable, might be susceptible to hydrogen-stress-induced cracking (HISC).

Due to its excellent resistance to localized corrosion and environmentally assisted cracking at elevated temperatures as well as high resilience to hydrogen-assisted cracking mechanisms, UNS<sup>(1)</sup> N08034 – a

---

<sup>(1)</sup> Unified Numbering System

© 2022 Association for Materials Protection and Performance (AMPP). All rights reserved. No part of this publication may be reproduced, stored in a retrieval system, or transmitted, in any form or by any means (electronic, mechanical, photocopying, recording, or otherwise) without the prior written permission of AMPP.

Positions and opinions advanced in this work are those of the author(s) and not necessarily those of AMPP. Responsibility for the content of the work lies solely with the author(s).

superaustenitic stainless steel with increased nickel content and balanced additions of nitrogen and manganese – is a promising candidate for oil and gas applications. Its refined chemical composition improves manufacturing characteristics to allow the fabrication of large components, including good machinability and weldability. Its non-magnetic nature enables the use in directional drilling and reservoir characterization tools. Since one limitation of austenitic stainless steels is their strength, cold working has been used to increase the yield strength of UNS N08034 to values higher than 120 ksi (827 MPa). In this study, a manufacturing process was developed based on thermodynamic and laboratory studies and subsequently applied to mill production trials. This paper reports the results from mechanical testing as well as microstructural investigations and corrosion testing conducted on strain-hardened UNS N08034.

Key words: UNS N08034, Strain-hardening, High Strength Super Austenitic Stainless Steel, Pitting Corrosion, oil and gas exploration, non-magnetic

## INTRODUCTION

Wells in oil, gas and geothermal production experience a broad spectrum of operating conditions in terms of temperature, depth, pressure and production environments, which govern material selection. For severe environments, where high strength and toughness combined with excellent corrosion and cracking resistance are required, a new superaustenitic stainless steel has been recently developed. Aiming for a minimum yield strength of at least 120 ksi (827 MPa), strain hardening enables the desired mechanical properties, allowing users to avoid well known but HISC susceptible and less cost effective precipitation hardened (PH) nickel alloys.

UNS N08034, commercially known as Alloy 31 Plus<sup>(2)</sup>, is a Nickel-Iron-Chromium-Molybdenum alloy, situated between the high-alloyed stainless steels and the Nickel-Chromium-Molybdenum alloys in terms of chemistry. UNS N08034 has controlled additions of nitrogen and optimized nickel content in comparison to its predecessor Alloy 31 (UNS N08031). The addition of nitrogen provides not only an increase in strength, but also an increase in the pitting corrosion resistance,<sup>1</sup> as expressed by its high Pitting Resistance Equivalent Number (PREN),<sup>2</sup> which is calculated at 54 according to Equation 1. A comparison of the corrosion resistance of UNS N08034 with other well-known solid solution alloys is published elsewhere.<sup>3</sup>

$$PREN = \% Cr + (3.3 \times \% Mo) + (16 \times \% N) \quad (\text{Eq. 1})$$

While nitrogen improves the strength and the corrosion resistance, the higher nickel content improves the metallurgical stability of the alloy. High-alloyed 6-Mo-stainless steels including UNS N08034 are usually prone to the precipitation of the detrimental tetragonal intermetallic sigma-phase, a chromium, molybdenum, nickel and iron containing phase which lowers environmental cracking resistance and toughness. An increase of about 3 % nickel in comparison to UNS N08031 is essential to the fabrication of large components of UNS N08034. It reduces the sigma-solvus temperature, allowing a solution annealing at 1140-1160 °C, and retards significantly the formation of sigma-phase, allowing the alloy a longer soak under critical temperatures before this detrimental phase precipitates. This makes UNS N08034 more convenient for manufacturing than UNS N08031, which requires higher heat treatment temperatures and faster cooling rates.<sup>1</sup> This feature is of great relevance mainly if heavy section products are to be manufactured, taking in consideration the limitations in terms of cooling rates after heat treatment.

Thus, UNS N08034 combines the advantages of high chromium and molybdenum containing materials, that is the high resistance to localized corrosion, allowing to create a highly corrosion resistant material

---

<sup>(2)</sup> Trade name. Alloy 31 Plus and Alloy 31 are proprietary alloys of VDM Metals International GmbH

© 2022 Association for Materials Protection and Performance (AMPP). All rights reserved. No part of this publication may be reproduced, stored in a retrieval system, or transmitted, in any form or by any means (electronic, mechanical, photocopying, recording, or otherwise) without the prior written permission of AMPP.

Positions and opinions advanced in this work are those of the author(s) and not necessarily those of AMPP. Responsibility for the content of the work lies solely with the author(s).

using only small amounts of expensive alloying elements.<sup>4</sup> In addition to its exceptional pitting and crevice corrosion resistance, high strength and high toughness can be achieved through strain hardening processes, which allows the alloy to be used in several applications including those relevant to the oil and gas industry, e.g. completions and production tools, subsea and wellhead equipment and, especially, directional drilling and reservoir characterization tools.

## EXPERIMENTAL PROCEDURES FOLLOWED

### Thermodynamic calculations

Thermodynamic calculations were carried out using the software Thermocalc<sup>(3)</sup> Version 2021a, Data base TCFE 9 in order to define manufacturing temperature windows, to avoid an unwanted precipitation of detrimental phases. A nominal chemical composition of UNS N08034 was used for the calculations.

### Material

Four heats of UNS N08034 within the nominal chemical composition given in **Table 1** were used for the investigation program. The heats were melted in an electric furnace, followed by vacuum degassing and electro-slag-remelting (ESR). The ESR process removes macrosegregation, ensuring a cleaner and more homogeneous ingot, with fewer non-metallic inclusions compared to a cast product.<sup>5</sup>

**Table 1**  
**Nominal chemical composition (in wt.%) of Alloy UNS N08034**

	Ni	Cr	Fe	S	Si	Mn	P	Mo	Cu	N	C	Al
Min	33.5	26.0	Bal.			1.0		6.0	0.5	0.10		
Max	35.0	27.0		0.01	0.1	4.0	0.02	7.0	1.5	0.25	0.01	0.30

The ESR ingots were pre-forged at high temperature to achieve the desired diameters of pre material. After forging, the ingots were solution annealed followed by rapid cooling in a water bath in order to avoid sigma-phase precipitation. The transport from heat treatment furnace to water quenching is critical and must be conducted quickly. After annealing, the billets were peeled and then strain-hardened through a rotary forging process at a controlled temperature.

Heats A, B, C and D were forged to different and increasing cold work ratios, in which heat A was subjected to the lowest amount of cold work and heat D to the highest amount.

After final surface preparation, the bars had diameters of about 200 mm (7.9").

### Mechanical Properties and Microstructure

Specimens for hardness, tensile and impact energy tests were taken in the center, at mid-radius and at 1" (25.4 mm) below surface from both the top and the bottom of the bars.

<sup>(3)</sup> Tradename.

© 2022 Association for Materials Protection and Performance (AMPP). All rights reserved. No part of this publication may be reproduced, stored in a retrieval system, or transmitted, in any form or by any means (electronic, mechanical, photocopying, recording, or otherwise) without the prior written permission of AMPP.

Positions and opinions advanced in this work are those of the author(s) and not necessarily those of AMPP. Responsibility for the content of the work lies solely with the author(s).

## Hardness

The Rockwell C hardness (HRC) of the produced bars was measured according to ASTM E18<sup>6</sup>.

## Tensile Testing

Tensile testing was carried out according to ASTM E8<sup>7</sup> at room temperature (RT) using round tensile specimens. Additionally, heat D was tested at RT in the transversal direction and according to ASTM E21<sup>8</sup> at 205 °C (401 °F) in the longitudinal and transversal directions.

## Impact Energy Testing

Charpy V-notched impact energy specimens were tested in the longitudinal direction at RT according to ASTM E23<sup>9</sup>.

## Microstructure

The microstructure of the finished material was analyzed using optical metallographic methods on samples taken from the region close to the surface of the bars, at 1" (25.4 mm) below surface. The samples were etched by immersion method in a nitric acid-hydrochloride 6:1 solution.

The grain size was determined using ASTM<sup>4</sup> E112<sup>10</sup>.

## **Corrosion Resistance**

The corrosion resistance of the strain-hardened bars of Alloy UNS N08034 was also investigated. The critical pitting temperature (CPT) and critical crevice temperature (CCT) in acidified ferric chloride solution were measured according to ASTM G48<sup>11</sup> Methods C and D, respectively. The standard testing period of 72 hours was used. The intergranular corrosion resistance in boiling ferric sulfate-sulfuric acid solution was measured using ASTM G28<sup>12</sup> Method A.

Additionally, the susceptibility to pitting corrosion in the "green death" solution was measured. The testing procedure to define the CPT was the same as described in ASTM G48 Method C, but using a solution containing 7% sulfuric acid, 3% hydrochloric acid, 1% iron chloride and 1% copper chloride, so called "green death", which is more aggressive than the standard ferric chloride solution.

Two test iterations were performed per heat tested and the samples for corrosion testing were taken from 1" (25.4 mm) below surface. For the CPT and CCT tests, new samples were used for each new temperature tested, in order to avoid any "learning" effect.

## **RESULTS OF EXPERIMENTS**

### **Thermodynamic calculations**

The calculated phase diagram is shown on **Figure 1**.

It was determined that sigma-phase can precipitate in this alloy at temperatures roughly between 650 and 1100 °C (1202-2012 °F). Sigma-phase is well known as a detrimental phase, due to its high contents

---

<sup>4</sup> American Society for Testing and Materials (ASTM), West Conshohocken, Pennsylvania, US.

© 2022 Association for Materials Protection and Performance (AMPP). All rights reserved. No part of this publication may be reproduced, stored in a retrieval system, or transmitted, in any form or by any means (electronic, mechanical, photocopying, recording, or otherwise) without the prior written permission of AMPP.

Positions and opinions advanced in this work are those of the author(s) and not necessarily those of AMPP. Responsibility for the content of the work lies solely with the author(s).

of molybdenum and chromium, which depletes these both alloying elements from the surrounding matrix, causing a local reduction of the nobility, reducing corrosion resistance and toughness.

With that knowledge, the manufacturing route should avoid processing the material in this range, and any process performed at temperatures higher than 1100 °C (2012 °F) should be followed by a rapid cooling to temperatures below 650 °C (1202 °F).

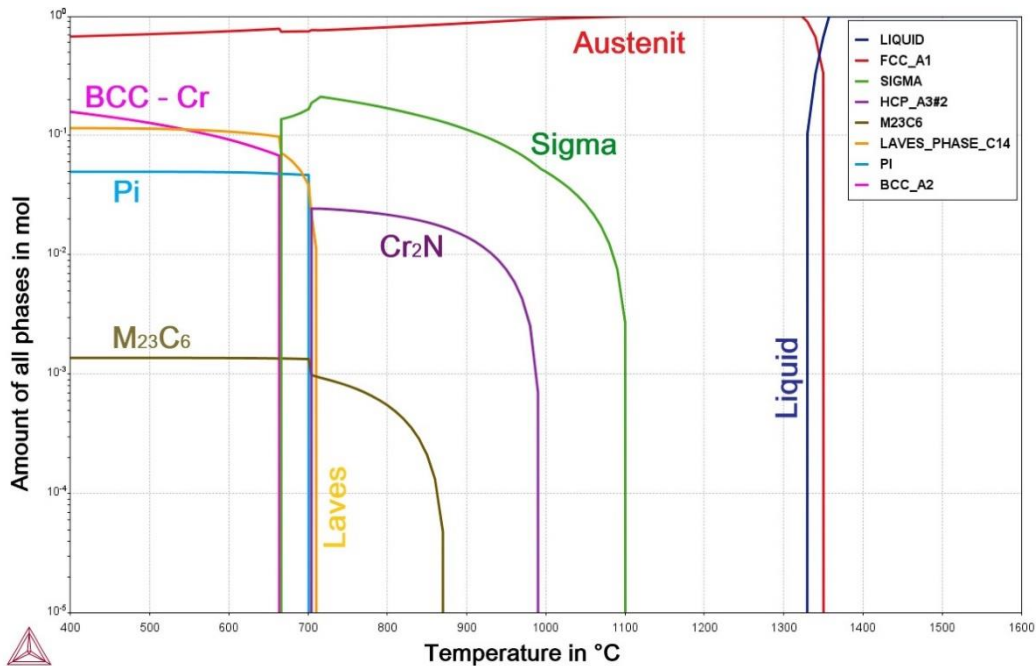


Figure 1: Phase diagram of UNS N08034 calculated using the software Thermocalc

## Mechanical Properties and Microstructure

### Mechanical Properties – Hardness, Tensile and Charpy Impact

In terms of simplification, the results from hardness, tensile and impact testing are provided as averages for each testing position and shown on **Table 2**. **Figure 2** shows the tensile properties in the graphical format.

As the cold working ratio increases, as expected, the material’s strength also increases. With the smaller amount of strain-hardening (Heat A), the achieved yield and tensile strengths are about 100 ksi (689 MPa) and 120 ksi (827 MPa), respectively. With this low forming ratio, it could be demonstrated that between the center and the surface of the bar there is some difference in the mechanical properties. By the next increase of the cold work ratio (heat B), the impact on the strengths and ductility is not relevant. A bigger impact of the forming ratio on the mechanical properties is drastically seen at higher forming ratios, as the used to produce heats C and D. At the third cold work ratio tested (heat C), the yield and tensile strengths increase to about 120 ksi (827 MPa) and 140 ksi (965 MPa), respectively and the elongation, as a result, drops to about 30 %. At the highest tested cold work (heat D), a yield strength above 140 ksi (965 MPa) and a tensile strength above 150 ksi (1034 MPa) were achieved. The elongation slightly drops to about 20 %, which still may be acceptable for many applications. At this level of cold work, the mechanical properties are constant in the whole cross section of the bar.

Increasing the cold working ratio lowers Charpy toughness, which, however, remains as high as about 148 tf-lbs (200 J) even at the highest amount of cold work and consequently highest strength.

**Table 2**

**Average mechanical properties of heats A, B, C and D of UNS N08034. Each heat was forged to different and increasing cold work ratios, where heat A was submitted to the lowest amount of cold work and heat D to the highest one.**

Heat	test position	Hardness (HRC)	Tensile				Impact Energy	
			RoA (%)	Elong. 4D (%)	YS ksi(MPa)	UTS ksi(MPa)	Impact energy ft-lbs (J)	Lateral Expansion in. (mm)
A	1" below surf.	25.7	71	39	106(730)	126(868)	236(320)	0.083(2.1)
	Mid-radius	22.9	60	38	101(697)	126(868)	216(293)	0.081(2.1)
	Center	20.1	62	46	91(628)	122(843)	254(344)	0.080(2.0)
B	1" below surf.	25.2	71	37	107(735)	127(877)	212(287)	0.080(2.0)
	Mid-radius	23.1	68	38	105(726)	128(881)	219(297)	0.084(2.1)
	Center	21.0	65	43	97(667)	125(864)	201(273)	0.081(2.1)
C	1" below surf.	29.2	58	27	121(834)	140(967)	129(175)	0.065(1.6)
	Mid-radius	28.2	59	32	117(807)	137(946)	129(175)	0.062(1.6)
	Center	25.3	56	35	109(753)	134(924)	121(164)	0.063(1.6)
D	1" below surf.	31.8	67	21	147(1016)	160(1104)	148(201)	0.072(1.8)
	Mid-radius	30.2	61	19	144(995)	157(1086)	147(199)	0.070(1.8)
	Center	27.3	64	20	147(1014)	153(1057)	145(196)	0.070(1.8)

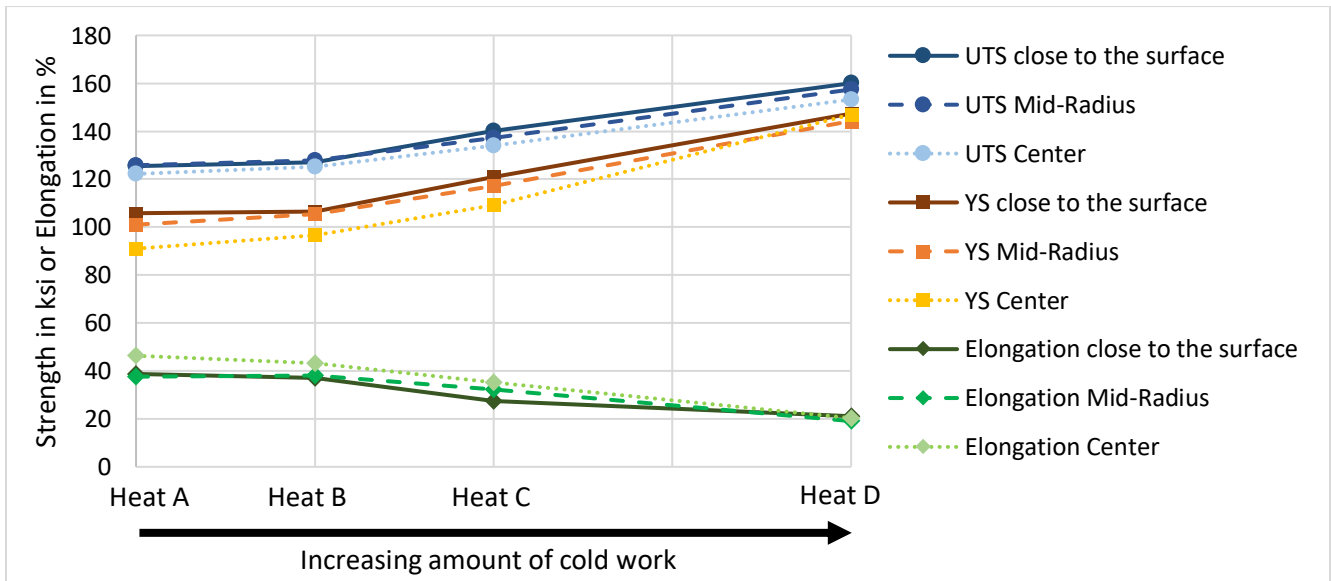


**Figure 2: Diagram showing the tensile properties of all four produced heats of Alloy UNS N08034. Samples were taken close to the surface, on the mid-radius and on the center of the produced bars. Tensile strength and yield strength are given in ksi and Elongation is given in %.**

The heat D was additionally tested in the transversal direction and at temperature (205 °C / 401 °F). The results are shown on **Table 3**. The material has comparable properties in both transversal and longitudinal directions. With the temperature increase to 205 °C (401 °F), the yield strength drops to about 113 ksi (779 MPa) and the tensile strength to about 127 ksi (876 MPa).

**Table 3**  
**Average tensile properties of heat D of UNS N08034 in the longitudinal direction at RT and in the transversal direction at RT and at 205 °C (401 °F)**

Heat	sample orientation	Test Temperature °C(°F)	Tensile			
			RoA (%)	Elong. 4D (%)	YS ksi(MPa)	UTS ksi(MPa)
D	transversal	RT	70.9	21.4	145(998)	161(1111)
	transversal	205(401)	71.2	20.6	113(780)	127(873)
	longitudinal	205(401)	68.0	18.6	114(786)	127(876)

Microstructure

Photomicrographs of heat D are shown in **Figure 3** as an example for the alloy microstructure after forging with higher cold working ratios. The manufacturing parameters produce an austenitic microstructure free of sigma-phase. The microstructure of the other produced heats appeared similar, but are not shown, as the desired mechanical properties were not achieved.

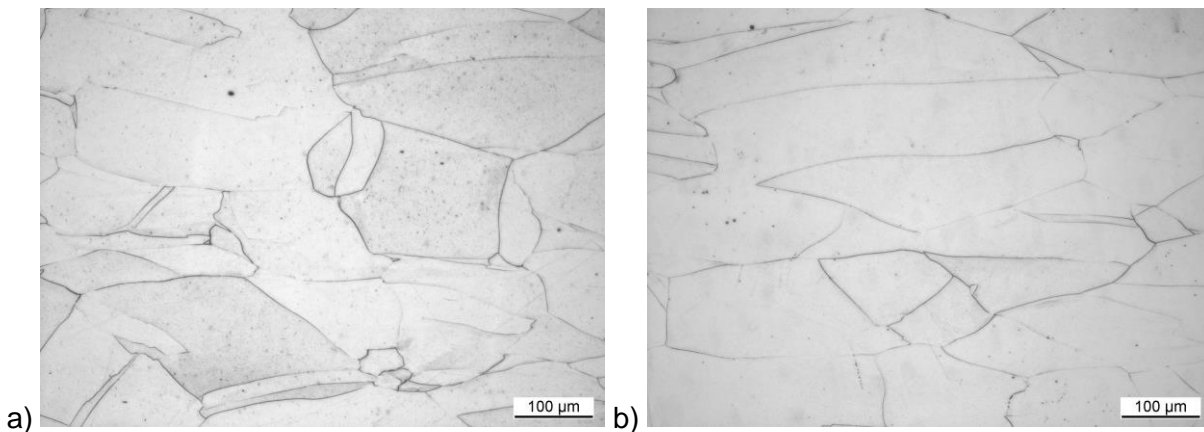


**Figure 3: Photomicrographs of UNS N08034, heat D, a) from the top and b) from the bottom of the bar, at 1” (25.4 mm) below surface at 100X magnification**

**Corrosion Resistance**

The CPT and CCT of samples from Heat D determined according to ASTM G48 C and D, respectively, are shown in **Table 4**. Values of CPT and CCT from annealed material in literature<sup>13</sup> were added to the table for comparison, noting that Behrens et al. reported the CCT defined on the same sample used for testing at the next higher temperatures. ASTM G48 states that new specimens and freshly prepared solution should be used for each temperature tested.

The strain-hardening process did not have a significant influence on CPT compared with solution annealed material. However, CCT slightly decreased.

© 2022 Association for Materials Protection and Performance (AMPP). All rights reserved. No part of this publication may be reproduced, stored in a retrieval system, or transmitted, in any form or by any means (electronic, mechanical, photocopying, recording, or otherwise) without the prior written permission of AMPP. Positions and opinions advanced in this work are those of the author(s) and not necessarily those of AMPP. Responsibility for the content of the work lies solely with the author(s).

**Table 4**  
**Critical Pitting Temperature (CPT) and Critical Crevice Temperature (CCT) of Heat D of cold worked UNS N08034 tested according to ASTM G48 Methods C and D**

Heat	Sample	CPT °C(°F)	CCT °C(°F)
D	D1	90(194)	55(131)
	D2	90(194)	55(131)
UNS N08034 Literature (12) in the solution-annealed condition		90(194)	70(158)

Other commonly used alloys in oil and gas components have lower corrosion resistance. There is limited information regarding the CPT and CCT of well-known precipitation hardened Alloy 718 (UNS N07718) and Alloy 925 (UNS N09925) in literature and in datasheets. According to available information, Alloy 718 has a CPT that varies from of 20 to 45 °C (68 to 113 °F) and a CCT that varies from 5 to 30 °C (41 to 86 °F), and Alloy 925 has a CPT of 30 to 35 °C (86 to 95 °F) and CCT of < 0 °C (32 °F).<sup>14-16</sup> Strain hardened Alloy UNS N08034 has demonstrated superior pitting and crevice corrosion resistance compared to both PH Ni-alloys.

Note that the iron chloride solution typically chemically decomposes at temperatures around 85 °C (185 °F), which is therefore the maximum temperature of test suggested in the ASTM G48 C specification.

The intergranular corrosion rates of samples from Heat D in the annealed condition according to ASTM G28 Method A are shown in **Table 5**. Behrens et al.<sup>13</sup> mentions that UNS N08034 does not show sensitization behavior even after exposure to 675 °C (1247 °F) for 24 hours. The corrosion rates achieved by strain-hardened UNS N08034 tested for 120 hours were lower than the values obtained for solution-annealed material available in the literature. The corrosion rate of this material published in the literature was obtained after a test period of 24 hours, while cold worked UNS N08034 was tested for a period of 120 hours.

It is known that UNS N08034 tested according to ASTM G28 A may present a “learning effect” that would result in lower corrosion rates after testing for longer periods. The results demonstrate that, independent of testing duration, UNS N08034 shows very low corrosion rates, indicating that no detrimental phases causing Cr-depletion are precipitated along grain boundaries during the production process.

**Table 5**  
**Intergranular corrosion rates of samples of heat D of cold worked UNS N08034 tested according to ASTM G28 Practice A**

Heat	Sample	Test duration (h)	Corrosion rate (mm/a)
D	DA1	120	0.13
	DA2	120	0.15
UNS N08034 Literature (12) in the solution-annealed condition		24	0.22

The susceptibility to pitting corrosion in the “green death” solution is shown in **Table 6**. The two samples GT1 and GT2 had Critical Pitting Temperatures of 55 °C (131 °F) and 65 °C (149 °F), respectively. These values are still somewhat lower than the CPT of annealed material from the literature.<sup>13</sup> This can be an effect of the use of fresh samples for each test cycle, or an effect of the cold

© 2022 Association for Materials Protection and Performance (AMPP). All rights reserved. No part of this publication may be reproduced, stored in a retrieval system, or transmitted, in any form or by any means (electronic, mechanical, photocopying, recording, or otherwise) without the prior written permission of AMPP.

Positions and opinions advanced in this work are those of the author(s) and not necessarily those of AMPP. Responsibility for the content of the work lies solely with the author(s).

working condition. However, the difference between could also be considered to be within the normal variation that the test produces. A deeper investigation of sample D GT 1 may be required to understand the reason for the lower corrosion resistance in comparison to sample D GT 2.

**Table 6**  
**CPT of UNS N08034 in the cold worked condition per ASTM G48 Method C in the “Green Death” solution**

Heat	Sample	CPT °C(°F)
D	D GT 1	55(131)
	D GT 2	65(149)
UNS N08034 from Literature (12)		75(167)

### CONCLUSIONS

- UNS N08034 having high strength can be manufactured by means of strain-hardening at sizes up to 200 mm (7.9”). Material cold worked in the context of these studies has reached a yield strength above 140 ksi (965 MPa).
- Strain-hardened Alloy UNS N08034 shows an interesting combination of mechanical properties and corrosion resistance that enables its use in oil and gas applications including directional drilling and reservoir characterization tools, completion and production equipment, as well as subsea and wellhead components.
- If enough cold working is applied, the material is mechanically conformed homogeneously from mid-radius outward. No significant gradient of properties could be detected in the cross section of the produced bars.
- The corrosion resistance of strain-hardened Alloy UNS N08034 is comparable to the corrosion resistance of standard solution-annealed material and is higher than and the commonly used PH Ni-alloys.

### ACKNOWLEDGEMENTS

The authors would like to thank Sebastian Maus from the corrosion laboratory of VDM Metals International GmbH for carrying out all of the corrosion testing presented in this paper, and to VDM Metals International GmbH, Deutsche Edelstahlwerke Specialty Steel GmbH & Co. KG and Baker Hughes for allowing us to present the results.

### REFERENCES

1. Alves, Helena et al. *Evolution of Nickel Base Alloys - Modification to Traditional Alloys for Specific Applications*. San Antonio, TX, USA : NACE International, 2014. Paper No. 4317.
2. NACE MR0175/ISO 15156-2015 "Petroleum and natural gas industries - Materials for use in H2S-containing environments in oil and gas production". Houston, TX : NACE International, 2015.

3. Niespodziany, Daniela et al. *Characterization of novel high performance material UNS N08034*. Nashville, TN : NACE International, 2019. Paper No. 13156.
4. Alves, Helena et al. *Recent Experiences with UNS N08031 Plus Roll Bond Cladding*. New Orleans, Louisiana, USA : NACE International, 2017. Paper No. 9470.
5. Reed, R. C. *The Superalloys: Fundamentals and Applications*. Cambridge University Press. 2006.
6. *ASTM E18-20, Standard Test Methods for Rockwell Hardness of Metallic Materials*. West Conshohocken, PA : ASTM International, 2020.
7. *ASTM E8 / E8M-21, Standard Test Methods for Tension Testing of Metallic Materials*. West Conshohocken, PA : ASTM International, 2021.
8. *ASTM E21, Standard Test Methods for Elevated Temperature Tension Tests of Metallic Materials*. West Conshohocken, PA : ASTM International, 2017.
9. *ASTM E23-18, Standard Test Methods for Notched Bar Impact Testing of Metallic Materials*. West Conshohocken, PA : ASTM International, 2018.
10. *ASTM E112-13, Standard Test Methods for Determining Average Grain Size*. Conshohocken, PA : International, ASTM, 2013.
11. *ASTM G48-11(2020)e1, Standard Test Methods for Pitting and Crevice Corrosion Resistance of Stainless Steels and Related Alloys by Use of Ferric Chloride Solution*. West Conshohocken, PA : ASTM International, 2020.
12. *ASTM G28-02(2015), Standard Test Methods for Detecting Susceptibility to Intergranular Corrosion in Wrought, Nickel-Rich, Chromium-Bearing Alloys*. West Conshohocken, PA : ASTM International, 2015.
13. Behrens, R. et al. *New developed 6-Mo super austenitic stainless steel with low sigma solvus temperature and high resistance to localized corrosion*. Orlando, FL : NACE International, 2013. Paper No. 2228.
14. Maher. *Alloy 718 Data Sheet*. 2020. Rev 01.
15. Metals, Special. *High-Performance Alloys for Resistance to Aqueous Corrosion*. 200. SMC-026.
16. *ASTM A262-15, Standard Practices for Detecting Susceptibility to Intergranular Attack in Austenitic Stainless Steels*. Conshohocken, PA : ASTM International, 2015.